

# ***Irradiation Testing of a SiC/SiC Channel Box in the High Flux Isotope Reactor***

**Nuclear Technology  
Research and Development**

Approved for public release.  
Distribution is unlimited.

***Prepared for  
U.S. Department of Energy  
Nuclear Technology R&D  
Advanced Fuels Campaign***

***Authors:  
Christian M. Petrie, Kurt R. Smith,  
Joseph R. Burns, Annabelle G. Le Coq,  
Yutai Katoh, Christian P. Deck  
Oak Ridge National Laboratory***



***September 2018  
M3NT-18OR020203042***



#### **DISCLAIMER**

This information was prepared as an account of work sponsored by an agency of the U.S. Government. Neither the U.S. Government nor any agency thereof, nor any of their employees, makes any warranty, expressed or implied, or assumes any legal liability or responsibility for the accuracy, completeness, or usefulness, of any information, apparatus, product, or process disclosed, or represents that its use would not infringe privately owned rights. References herein to any specific commercial product, process, or service by trade name, trade mark, manufacturer, or otherwise, does not necessarily constitute or imply its endorsement, recommendation, or favoring by the U.S. Government or any agency thereof. The views and opinions of authors expressed herein do not necessarily state or reflect those of the U.S. Government or any agency thereof.



## **ACKNOWLEDGEMENTS**

This research was sponsored by the Advanced Fuels Campaign (AFC) Program of the US Department of Energy (DOE), Office of Nuclear Energy. Neutron irradiation in the High Flux Isotope Reactor (HFIR) is made possible by the Office of Basic Energy Sciences, US DOE. The report was authored by UT-Battelle under Contract No. DE-AC05-00OR22725 with the US Department of Energy.

## SUMMARY

This report provides a summary of the experiment design and the neutronics and structural analyses of a miniature SiC/SiC channel box that will be irradiated in the High Flux Isotope Reactor (HFIR). The goal of this experiment is to evaluate the lateral bowing in the channel box during irradiation under a radial neutron flux gradient. The concern is that lateral bowing could potentially block coolant flow or interfere with control blade movements in boiling water reactors (BWRs). The experiments described in this work will help validate thermomechanical models of channel box bowing. The experiment design allows for one channel box specimen to be irradiated in the HFIR while being directly cooled by the reactor coolant. Monte Carlo neutronics analyses are performed to determine the three-dimensional profile of the dose rate in the channel box. Dose is then converted to volumetric swelling, using literature data, and the resulting swelling profile is used as an input to structural finite element calculations that predict lateral bowing.



## CONTENTS

|                                    |     |
|------------------------------------|-----|
| ACKNOWLEDGEMENTS .....             | iii |
| SUMMARY .....                      | iv  |
| FIGURES .....                      | vii |
| ACRONYMS .....                     | ix  |
| 1. INTRODUCTION .....              | 1   |
| 2. Experiment Design Concept ..... | 1   |
| 2.1 HFIR Experiment Facility ..... | 1   |
| 2.2 Experiment Design .....        | 2   |
| 3. Computational Methods .....     | 3   |
| 3.1 Neutronics Analysis .....      | 3   |
| 3.2 Structural Analysis .....      | 4   |
| 4. Analysis Results .....          | 6   |
| 4.1 Neutronic Analysis .....       | 6   |
| 4.2 Structural Analysis .....      | 9   |
| 5. Summary and Conclusions .....   | 12  |
| 6. Works cited .....               | 12  |



## **FIGURES**

|  |    |
|--|----|
| Figure 1. Experiment positions in the HFIR. ....   | 2  |
| Figure 2. Design of the channel box experiment. ....   | 3  |
| Figure 3. MCNP model of the channel box experiment in the HFIR. ....   | 4  |
| Figure 4. ANSYS model with displacement constraints and finite element mesh of the channel box experiment. ....  | 5  |
| Figure 5. Volumetric swelling vs. dose from previous HFIR irradiations of SiC performed at coolant temperature (~60°C) and a power law fit to the experimental data [12]. ....   | 6  |
| Figure 6. Midplane (Z = 0 mm) dose per cycle as a function of X and Y using BOC and EOC HFIR models. ....  | 7  |
| Figure 7. Dose per cycle using BOC HFIR model as a function of axial position Z with Y as a parameter. ....  | 7  |
| Figure 8. Dose per cycle using EOC HFIR model as a function of axial position Z with Y as a parameter. ....  | 8  |
| Figure 9. Volumetric swelling as a function of Z with Y as a parameter. ....   | 9  |
| Figure 10. Predicted lateral (in the Y direction) displacement, in meters, after one HFIR irradiation cycle (24 days). The visual deformation of the structure is artificially magnified by a factor 10 and the undeformed structure is shown as a wireframe. .... | 10 |
| Figure 11. Maximum predicted lateral bowing as a function of Z with irradiation time as a parameter. ....  | 10 |
| Figure 12. Cross-section of channel box irradiation experiment near the vertical midplane of the specimen. ....  | 11 |



## **ACRONYMS**

| <b>Acronym</b> | <b>Description</b>            |
|----------------|-------------------------------|
| 3D             | Three-dimensional             |
| BOC            | Beginning of cycle            |
| BWR            | Boiling Water Reactor         |
| EOC            | End of cycle                  |
| GA             | General Atomics               |
| HFIR           | High Flux Isotope Reactor     |
| ORNL           | Oak Ridge National Laboratory |
| SiC            | Silicon carbide               |
| VXF            | Vertical Experiment Facility  |



# IRRADIATION TESTING OF A SiC/SiC CHANNEL BOX IN THE HIGH FLUX ISOTOPE REACTOR

## 1. INTRODUCTION

Silicon carbide (SiC) fiber-reinforced, SiC ceramic matrix composites (SiC/SiC composites) are being considered for a wide variety of current and advanced reactor designs [1, 2]. These composites have shown high strength and stability under irradiation and at high temperatures, while minimizing neutron absorption [3-5]. In addition, their high melting point and their reduced steam oxidation kinetics make them a strong candidate for accident tolerant fuel cladding for light water reactor applications. More recently, there has been increased interest in the use of SiC/SiC composites to replace traditional zirconium alloy channel boxes in boiling water reactors (BWRs). In a BWR environment, the channel box can be exposed to a significant radial fast neutron flux gradient, particularly for fuel assemblies located near the core periphery. A radial fast neutron flux gradient will cause differential radiation-induced swelling. This differential swelling could result in significant lateral bowing of the channel box, which could potentially obstruct coolant flow or interfere with control blade movement.

To address this issue, finite element models have been developed to predict the extent of the lateral bowing of SiC/SiC components including a channel box and fuel cladding [6, 7]. However, to date there has been no experimental data to validate the thermomechanical models. This work describes an irradiation experiment to measure the lateral bowing of a miniature SiC/SiC channel box that is being fabricated by General Atomics (GA). The channel box will be irradiated in the reflector of the High Flux Isotope Reactor (HFIR) at Oak Ridge National Laboratory (ORNL). In the reflector positions, there exist significant radial fast neutron flux gradients to drive a swelling differential, inducing lateral bowing. The results of this experiment will be used to improve the understanding of SiC/SiC deformation, even though the irradiation will be conducted at HFIR coolant temperatures (50–60°C), as opposed to typical BWR temperatures. This report describes the design of the irradiation experiment including neutronic and structural analyses.

## 2. Experiment Design Concept

### 2.1 HFIR Experiment Facility

The HFIR is a beryllium-reflected, pressurized, light water-cooled and moderated flux trap-type reactor [8, 9]. The channel box experiment will be irradiated in a large Vertical Experiment Facility (VXF) in the HFIR reflector (labelled positions 6, 14, 16, 17, 19, and 21 in Figure 1). The experiment design (see section 2.2) allows for the miniature channel box specimen to be directly cooled by the reactor coolant, which flows through the experiment from top to bottom at a temperature in the range of 50–60°C. The channel box specimen will be irradiated for 1 HFIR cycle, which has a typical duration of 24 days.

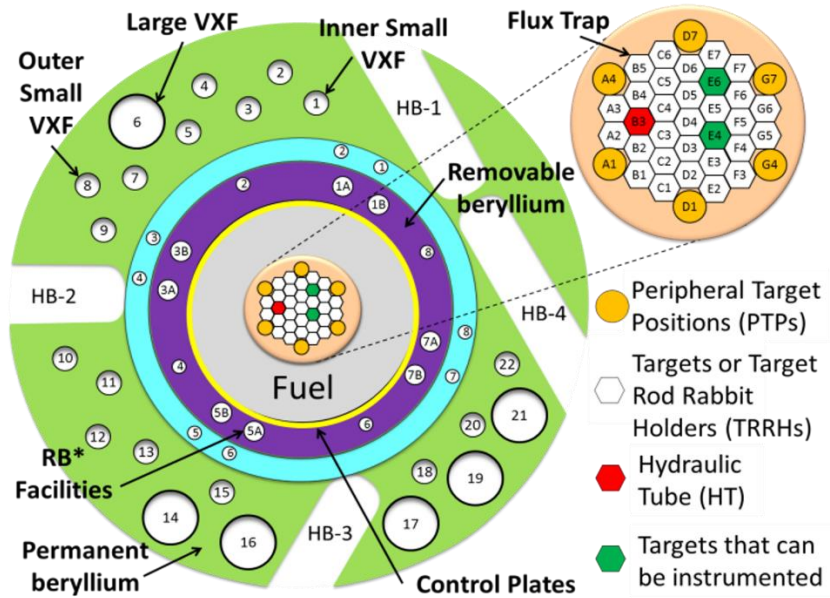


Figure 1. Experiment positions in the HFIR.

## 2.2 Experiment Design

The irradiation experiment design concept is shown in Figure 2. The irradiation vehicle is a two-piece aluminum holder that, when welded together, results in a cylindrical assembly with a square cutout. Holes at the top of the holder allow for the experiment to be lowered into the reactor using standard reactor operator tools. An orifice is welded to the bottom of the holder to prevent excessive flow through the assembly. The miniature channel box is assembled inside of the holder cutout. The nominal dimensions of the miniature channel box are  $30 \text{ mm} \times 30 \text{ mm} \times 0.38 \text{ m}$ , with a 1.25 mm wall thickness. Two aluminum support pieces, lower and upper, are stacked together on either end of the channel box and secured using a tie rod. The large features at the top and bottom of the support pieces ensure that the channel box remains centered inside the aluminum holder. Wave springs are placed between the channel box specimen and the supports to keep the channel box centered around the support pieces. The wave springs have minimal stiffness to allow the channel box to bow without applying any significant load, or stress on the channel box.

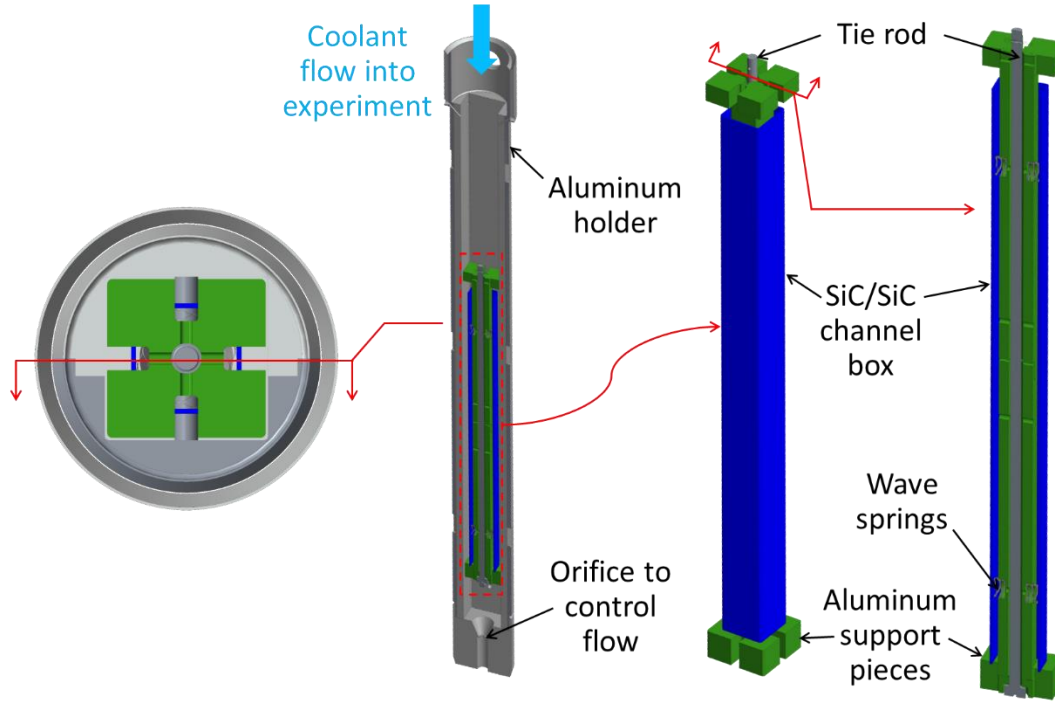


Figure 2. Design of the channel box experiment.

### 3. Computational Methods

#### 3.1 Neutronics Analysis

Neutronics analyses were performed to determine the spatial variation in dose rate within the channel box specimen to provide input to the subsequent structural analyses. Analyses were performed using the MCNP5 software code package. The MCNP calculations are based on existing fixed neutron source models of HFIR at beginning and end of cycle (BOC and EOC) with cycle 400 experimental loading [9]. Modifications were made to include the new experimental assembly inside VXF position 19, centered about the HFIR core midplane. A top-down cross section view of the channel box experiment as modeled is shown in Figure 3.

The channel box specimen dose is determined by tallying neutron flux in a Cartesian mesh superimposed over the experiment and applying a weighting multiplier as follows [10]:

$$\dot{d} = \frac{0.8}{2E_d} \int_0^\infty \phi(E) \sigma_d(E) dE \quad (1)$$

where  $\dot{d}$  is the dose rate,  $E_d$  is the average lattice displacement energy for SiC,  $\phi(E)$  is the energy-dependent neutron flux, and  $\sigma_d(E)$  is the energy-dependent radiation damage cross section for SiC. The factor of 0.8 is a representative displacement efficiency [10]. The lattice displacement energy for SiC is taken as 30 eV, which is the average of 40 eV for Si and 20 eV for C [11]. The integral quantity is assessed from the MCNP tally of neutron flux weighted by the radiation damage cross section from the standard MCNP cross section

libraries. In the absence of variance reduction techniques, statistical noise is minimized by running  $2 \times 10^{10}$  particle histories for each calculation, yielding uncertainties well within 5% across the entire calculation mesh.

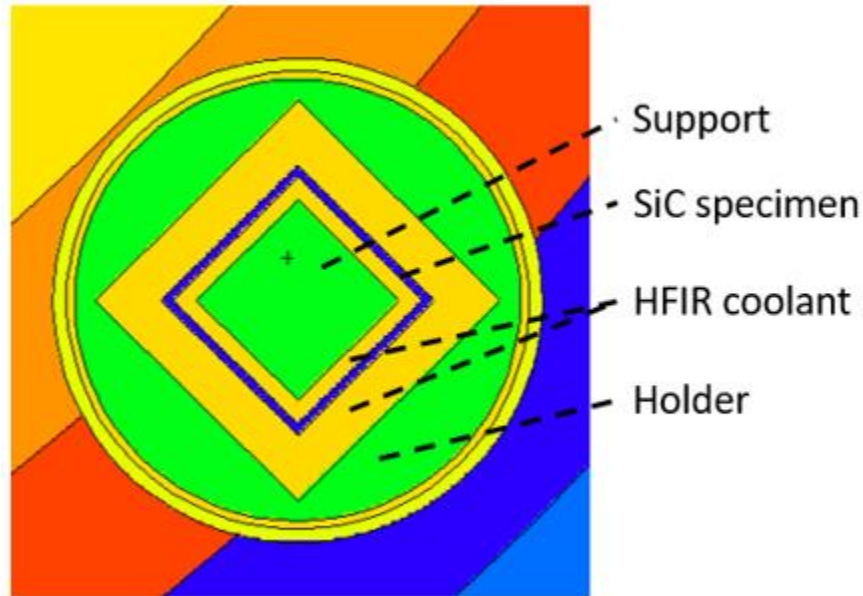


**Figure 3. MCNP model of the channel box experiment in the HFIR.**

### 3.2 Structural Analysis

A three-dimensional (3D) structural analysis was performed using the ANSYS finite element software package to estimate the bowing in the channel box during and after irradiation. The channel box experiment was modelled using a mesh size of 0.5 mm for the X and Y directions, and a 4-mm mesh size for the Z direction (see Figure 4). The origin is at the centroid of the channel box specimen. Figure 4 also shows how the channel box was constrained in the structural analysis. Symmetry was assumed along the YZ plane and displacement in the X direction ( $U_x$ ) was constrained along this plane. Along the XY plane, displacement in the Z direction ( $U_z$ ) was constrained. Finally, the channel box was constrained by setting the displacement in the Y direction ( $U_y$ ) equal to zero at a single point in the corner of the XY plane.



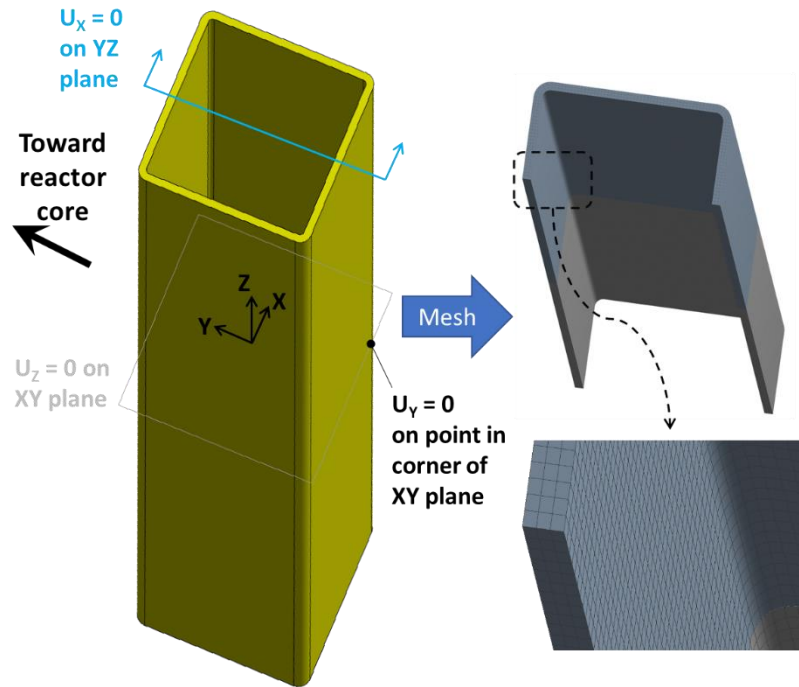


**Figure 4. ANSYS model with displacement constraints and finite element mesh of the channel box experiment.**

ANSYS has a built-in swelling model that requires the user to specify a spatially-dependent neutron fluence and an equation to convert from fluence to linear swelling. For this work, the dose rates determined in the neutronics analysis (see previous section) were multiplied by the simulated irradiation time to give total dose. Dose was converted to volumetric swelling using literature data from previous HFIR irradiation experiments performed at HFIR coolant temperatures [12]. The volumetric swelling was divided by a factor of 3 to convert to linear swelling (assumed isotropic swelling). Figure 5 shows the literature data along with a fit to the experimental data using a power law that was used to establish the dose-to-swelling model. It is important to note that the dose expected from one cycle of irradiation in a large VXF position in HFIR is expected to be below 0.05 dpa (see results in section 4.1). This dose range is between two of the three data points shown in Figure 5, which gives increased confidence in the validity of the dose-to-swelling model. Instead of inputting a representative neutron fluence profile into ANSYS, the linear swelling profile was imported into ANSYS as a neutron fluence and the fluence-to-swelling conversion was artificially set to one.

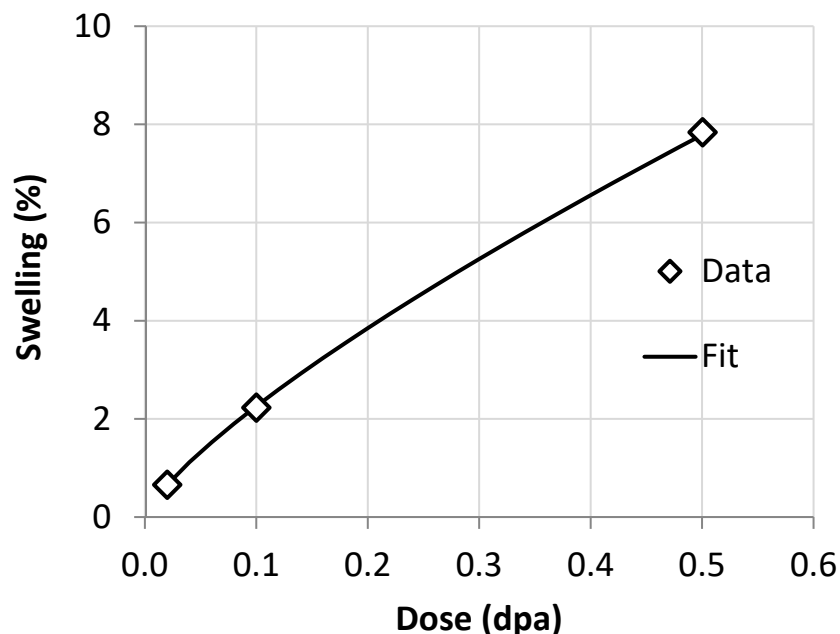


**Figure 5. Volumetric swelling vs. dose from previous HFIR irradiations of SiC performed at coolant temperature ( $\sim 60^{\circ}\text{C}$ ) and a power law fit to the experimental data [12].**

The structural analysis assumes an elastic modulus of 236 GPa for the channel box specimen. For this preliminary work, the effects of creep and pseudo-ductility due to microcracking were ignored. The calculation assumed a constant temperature of  $60^{\circ}\text{C}$ . Simulations were performed for various time steps over the course of one HFIR irradiation cycle (24 days).

## 4. Analysis Results

### 4.1 Neutronic Analysis

The spatially-dependent dose rate in the channel box specimen is shown in Figure 6 through Figure 8. Figure 6 shows the midplane ( $Z = 0$  mm) dose per cycle using BOC and EOC models as a function of X and Y position. This figure shows the significant reduction in dose when moving away from the HFIR core (decreasing Y). As expected, there is almost no dependence on X. Figure 7 shows dose per cycle using the BOC model as a function of Z for  $Y = 15$  mm (closest to the core),  $Y = 0$  mm (the center of the channel box, with respect to Y), and  $Y = -15$  mm (furthest from the core). Figure 8 shows the same dose per cycle data using the EOC model. These figures further illustrate the significant reduction in dose moving from the front to the back side of the channel box in the Y direction. The dose is reduced by approximately 33% over the 30 mm dimension of the channel box. There is also a significant dose dependence in the Z direction. The dose at the ends of the channel box ( $Z = \pm 190$  mm) is approximately 40% lower than the dose at the core midplane ( $Z = 0$  mm). Comparing Figure 7 and Figure 8, there are no significant differences in dose using the BOC vs. EOC model. This is expected considering this experiment is conducted far away from the HFIR control plates, which are gradually withdrawn throughout the HFIR cycle.

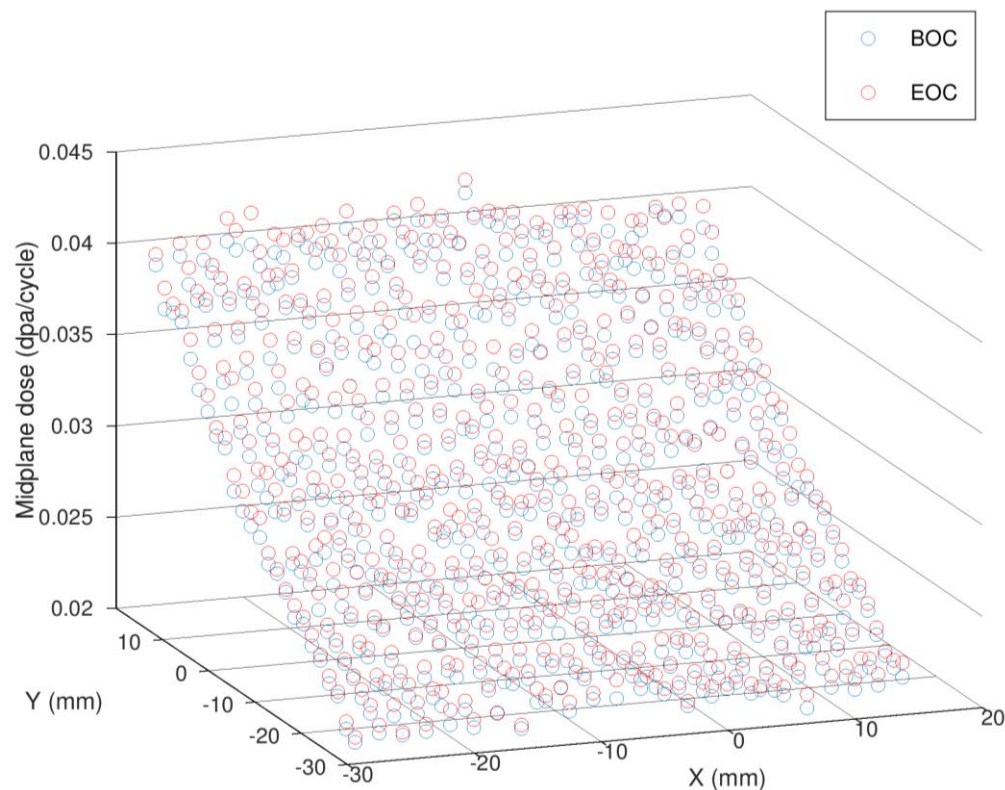


**Figure 6. Midplane ( $Z = 0$  mm) dose per cycle as a function of X and Y using BOC and EOC HFIR models.**

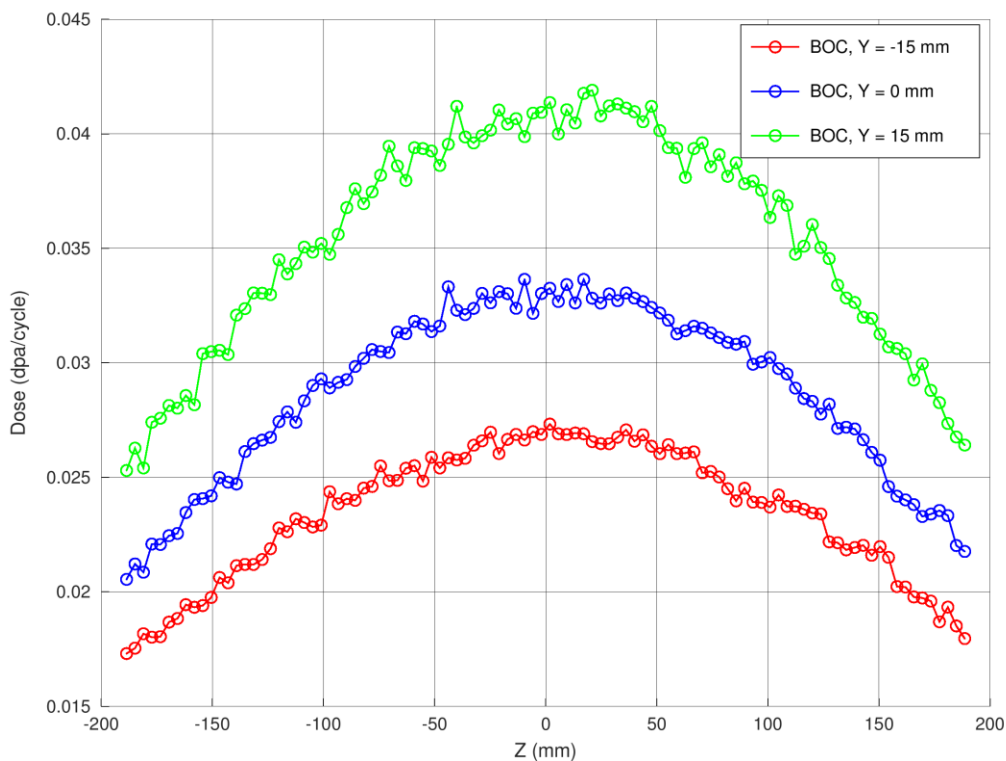


**Figure 7. Dose per cycle using BOC HFIR model as a function of axial position Z with Y as a parameter.**

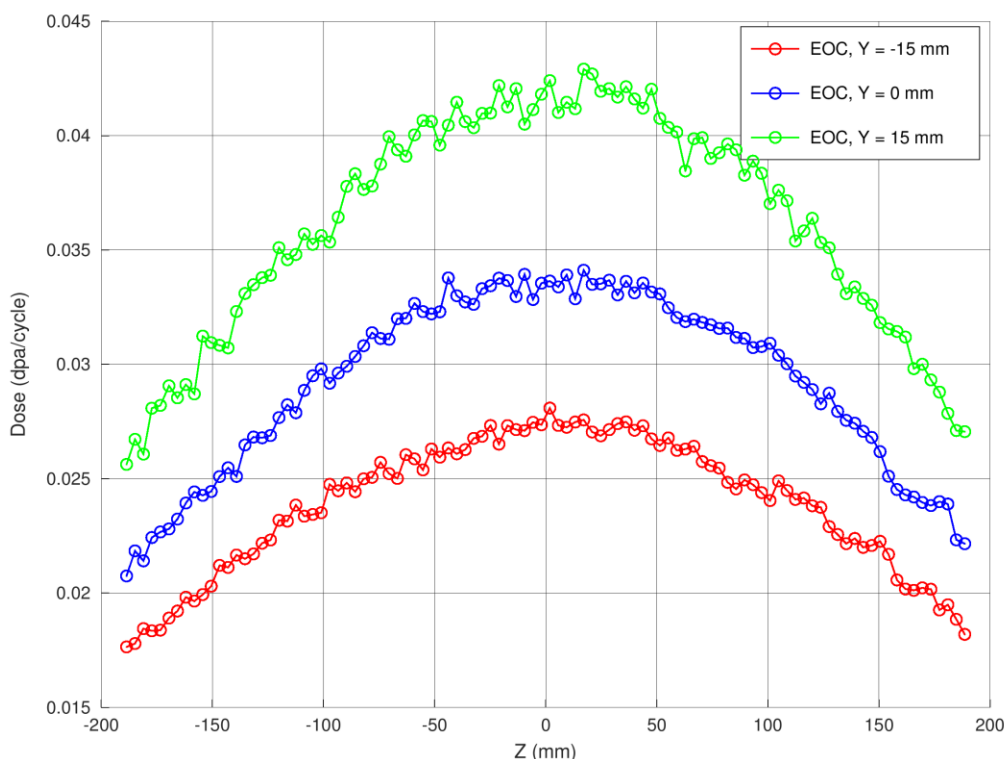


**Figure 8. Dose per cycle using EOC HFIR model as a function of axial position  $Z$  with  $Y$  as a parameter.**

Converting from dose to volumetric swelling using the model described in section 3.1 gives the results shown in Figure 9. Figure 9 shows volumetric swelling vs.  $Z$  with  $Y$  as a parameter. The dose used to determine the volumetric swelling used an average of the results obtained with the BOC and EOC models. Because the dose-to-swelling model is almost linear for dose ranging from 0 to 0.05 dpa, the variation in volumetric swelling (approximately 30%) from the front to the back side of the channel box is very similar to the variation in dose. Near the core midplane ( $Z = 0$  mm), the differential volumetric swelling is approximately 0.33%. The differential swelling decreases to approximately 0.2% near the ends of the channel box ( $Z = \pm 190$  mm).

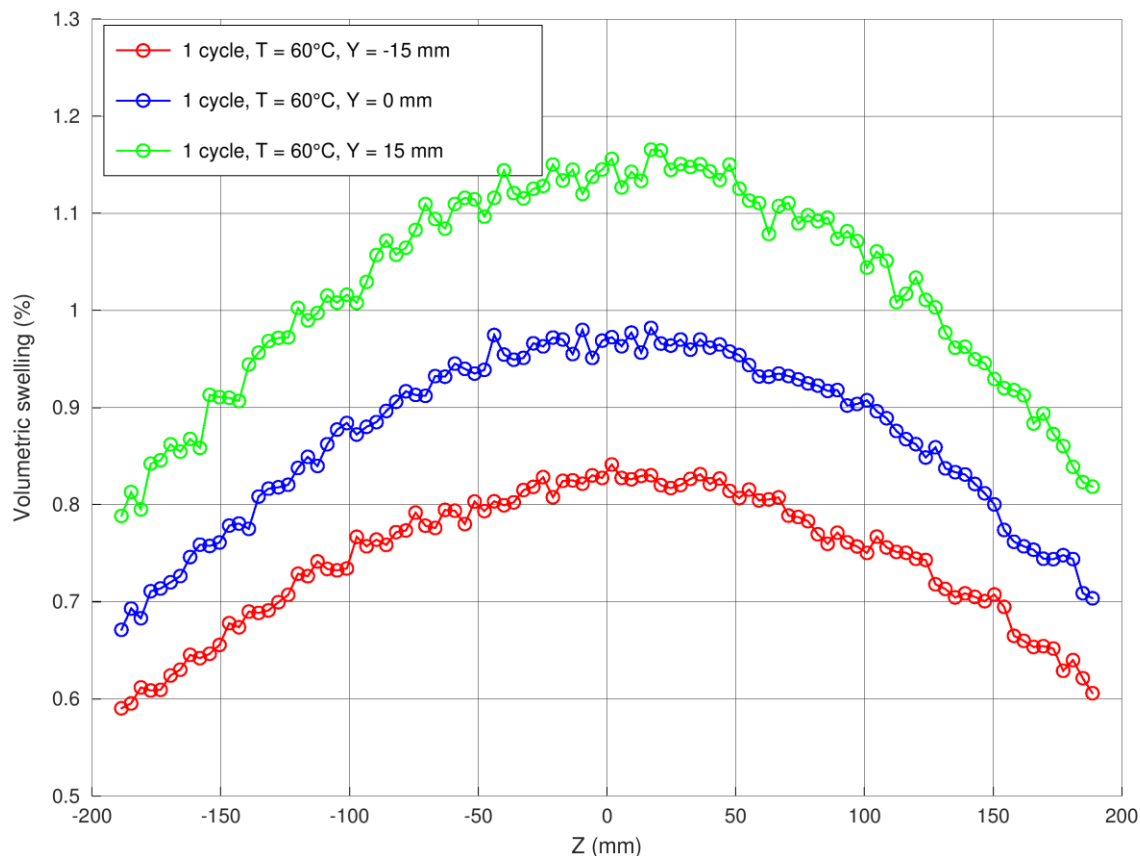
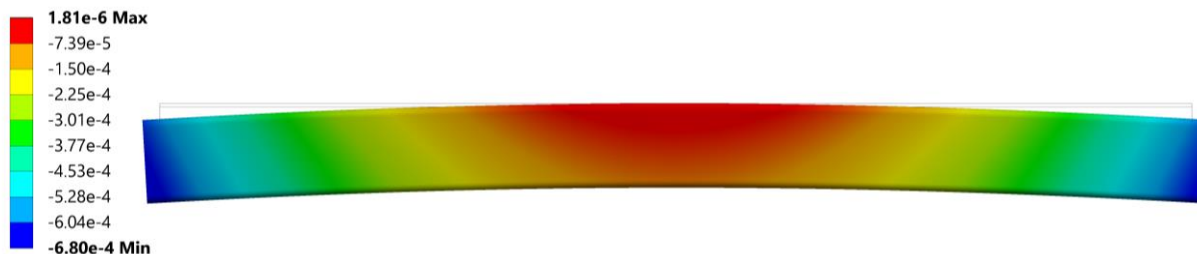


Figure 9. Volumetric swelling as a function of Z with Y as a parameter.

## 4.2 Structural Analysis

Figure 10 shows the predicted lateral (in the Y direction) displacement (in meters) in the channel box specimen over the course of one HFIR cycle (24 days). The visual deformation of the structure is artificially magnified by a factor 10 in this figure. The undeformed structure is shown as a wireframe. Figure 11 shows maximum lateral (in the Y direction) displacement as a function of Z, with the irradiation time as a parameter. The lateral bowing shown in Figure 11 is defined as the maximum lateral displacement for all nodes at a given Z position relative to the maximum lateral displacement at Z = 0 mm. In this way, the lateral bowing compensates for the swelling of the channel box in the Y direction. The lateral displacement in Figure 10 includes both the effects of bowing and swelling in the Y direction. This explains why the lateral displacement in Figure 10 (0.68 mm) is slightly larger than the lateral bowing (0.56 mm) in Figure 11 after 24 days of irradiation.



**Figure 10.** Predicted lateral (in the Y direction) displacement, in meters, after one HFIR irradiation cycle (24 days). The visual deformation of the structure is artificially magnified by a factor 10 and the undeformed structure is shown as a wireframe.

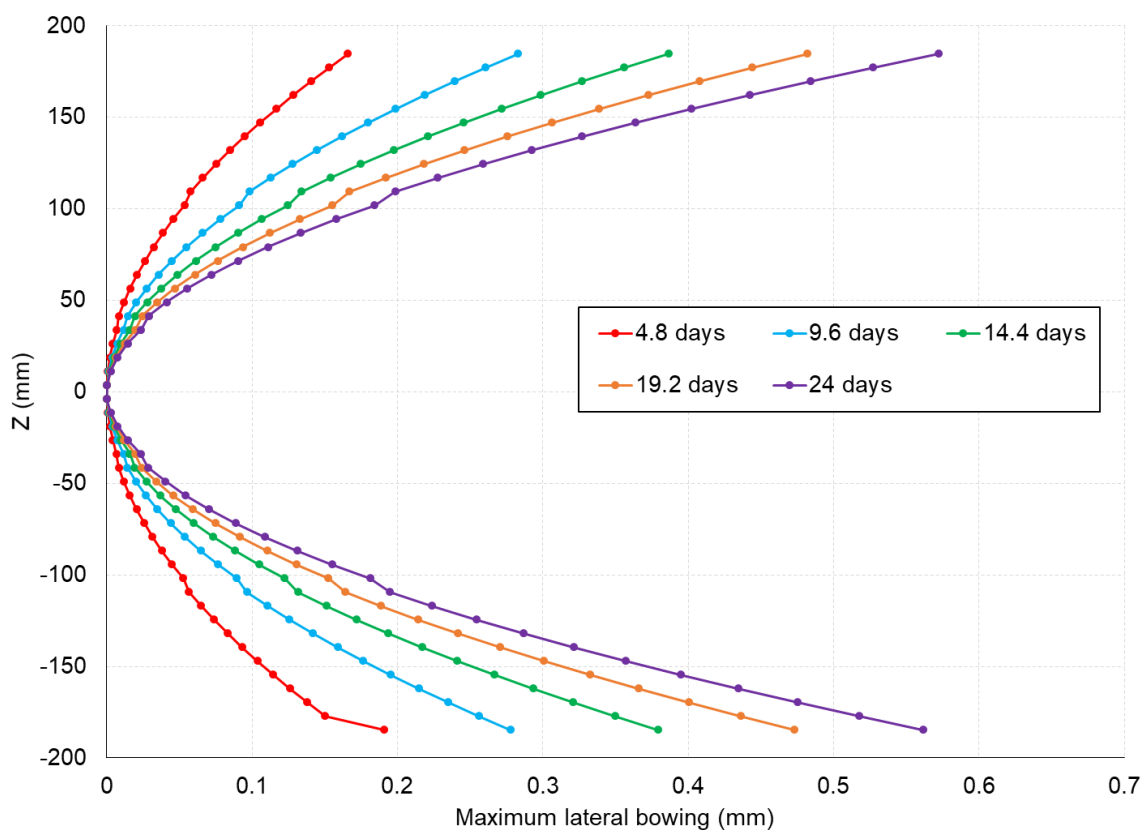


**Figure 11.** Maximum predicted lateral bowing as a function of Z with irradiation time as a parameter.

Figure 11 predicts a maximum lateral bowing of 0.56 mm. This amount of bowing can be measured without difficulty post-irradiation using laser profilometry. As a check, a first-order approximation to the lateral bowing can be made using the known dimensions and the differential volumetric swelling of 0.33% (0.11% linear swelling) at  $Z = 0$  mm. The channel box is constrained in the  $Z$  direction at the vertical midplane. Therefore, taking half the channel box height of 3.81 meters and multiplying by the differential linear swelling of 0.11% gives a differential expansion of 0.21 mm in the  $Z$  direction. The resulting deflection angle over the 30 mm width of the channel box is equal to  $\text{atan}\left(\frac{0.21 \text{ mm}}{30 \text{ mm}}\right) = 0.007$  rad. The radius of curvature for the bow is equal to  $\frac{30 \text{ mm}}{0.11\%} = 27.27$  m. With these parameters, the lateral bowing can be calculated as  $(27.27 \text{ m})(1 - \cos(0.007 \text{ rad})) = 0.67$  mm. It is not surprising that this simplistic analysis over-predicts the bowing because it does not consider the reduction of the differential swelling as the distance from the core vertical midplane increases.

The predicted bowing can be compared with the size of the flow channels in the HFIR experiment to determine whether there are any potential interference issues after bowing of the channel box specimens. Figure 12 shows a cross-sectional view of the experiment near the vertical midplane of the channel box specimen. The indicated 3.57 mm dimension is the limiting dimension that could result in interference if prohibitively large bowing of the channel box were to occur. However, this dimension is much larger than the maximum expected bowing. Therefore, no issues related to interference of the channel box specimen are expected.

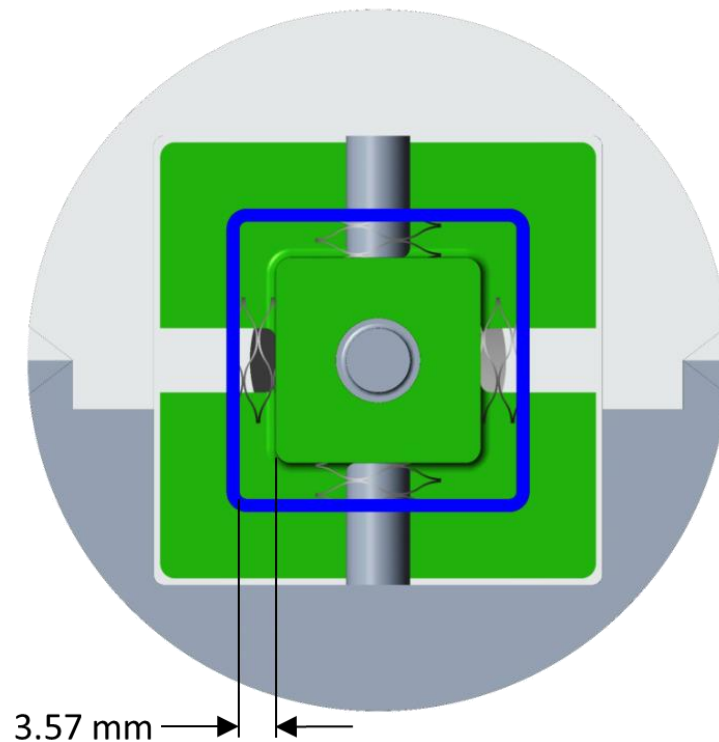


**Figure 12. Cross-section of channel box irradiation experiment near the vertical midplane of the specimen.**



## 5. Summary and Conclusions

This report presents the experiment design as well as the neutronic and structural analyses that support irradiation testing of a miniature SiC/SiC channel box. The channel box specimen will be irradiated for 1 cycle (about 24 days) in a large VXF position while being directly cooled by the reactor coolant, which remains at a temperature of approximately 50–60°C. The results of this experiment will be used for validation of thermomechanical models to predict channel box bowing, even though the irradiation will be conducted at lower temperatures compared to those of typical BWRs. The neutronics analyses predict a ~33% reduction in dose rate from the front face to the back face of the 30 mm wide channel box specimen. The structural analysis predicts bowing of 0.56 mm at the end of the irradiation. This amount of bowing is much less than the limiting coolant channel, which is nominally 3.57 mm, and the bowing can be measured using laser profilometry without much difficulty.

## 6. Works cited

1. C. Deck, G. Jacobsen, J. Sheeder, O. Gutierrez, H. Khalifa and C. Back, *Characterization of SiC-SiC Composites for Accident Tolerant Fuel*, Journal of Nuclear Materials, 2015, **466**: p. 667-681.
2. L.L. Snead et al, *Silicon carbide composites as fusion power reactor structural materials*, Journal of Nuclear Materials, 2011, **417**: p. 300-339.
3. Y. Katoh et al., *Radiation effects in SiC for nuclear structural applications*, Current Opinion in Solid State and Materials Science, 2012, **16**: p. 143-152.
4. Y. Katoh et al., *Current status and recent research achievements in SiC/SiC composites*, Journal of Nuclear Materials, 2016, **471**: p. 92-96.
5. T. Koyanagi, *Effects of neutron irradiation on mechanical properties of silicon carbide composites fabricated by nano-infiltration and transient eutectic-phase process*, Journal of Nuclear Materials, 2014, **448**: p. 478-486.
6. G. Singh, et al., *Parametric Evaluation of SiC/SiC Composite Cladding with UO<sub>2</sub> Fuel for LWR Applications: Fuel Rod Interactions and Impact of Nonuniform Power Profile in Fuel Rod*, Journal of Nuclear Materials, 2018, **499**: p. 155-167, DOI: <https://doi.org/10.1016/j.jnucmat.2017.10.059>.
7. Gyanender P. Singh, et al., *Preliminary Analysis of SiC BWR Channel Box Performance under Normal Operation*, ORNL/TM-2018/854, Oak Ridge National Laboratory, Oak Ridge, TN, 2018. <https://www.osti.gov/servlets/purl/1439933>.
8. *High Flux Isotope Reactor Technical Parameters*. Available from: <http://neutrons.ornl.gov/hfir/parameters>.
9. N. Xoubi and R.T. Primm III, *Modeling of the High Flux Isotope Reactor Cycle 400*, ORNL/TM-2004/251, Oak Ridge, TN, 2005.
10. E.A. Read, and C.R.E. de Oliveira. *A Functional Method for Estimating DPA Tallies in Monte Carlo Calculations of Light Water Reactors*. in M&C. 8-12 May 2011. Rio de Janeiro, Brazil.
11. S. J. Zinkle, *Defect Production in Ceramics*, Journal of Nuclear Materials, 1997, **251**: p. 200-217.
12. Lance L. Snead, et al., *Dimensional isotropy of 6H and 3C SiC under neutron irradiation*, Journal of Nuclear Materials, 2016, **471**: p. 92-96, DOI: <https://doi.org/10.1016/j.jnucmat.2016.01.010>.